The Astrophysical Journal, 836:205 (6pp), 2017 February 20 doi:10.3847/1538-4357/836/2/205

A Luminous and Isolated Gamma-Ray Flare from the Blazar B2 1215+30

A. U. Abeysekara[1], S. Archambault[2], A. Archer[3], W. Benbow[4], R. Bird[5], M. Buchovecky[6], J. H. Buckley[3], V. Bugaev[3], K. Byrum[7], M. Cerruti[4], X. Chen[8,9], L. Ciupik[10], W. Cui[11,12], H. J. Dickinson[13], J. D. Eisch[13], M. Errando[3,14], A. Falcone[15], Q. Feng[11], J. P. Finley[11], H. Fleischhack[9], L. Fortson[16], A. Furniss[17], G. H. Gillanders[18], S. Griffin[2], J. Grube[10], M. Hütten[9], N. Håkansson[8], D. Hanna[2], J. Holder[19], T. B. Humensky[20], C. A. Johnson[21], P. Kaaret[22], P. Kar[1], M. Kertzman[23], D. Kieda[1], M. Krause[9], F. Krennrich[13], S. Kumar[19], M. J. Lang[18], G. Maier[9], S. McArthur[11], A. McCann[2], K. Meagher[24], P. Moriarty[18], R. Mukherjee[14], T. Nguyen[24], D. Nieto[20], R. A. Ong[6], A. N. Otte[24], N. Park[25], V. Pelassa[4], M. Pohl[8,9], A. Popkow[6], E. Pueschel[5], J. Quinn[5], K. Ragan[2], P. T. Reynolds[26], G. T. Richards[24], E. Roache[4], C. Rulten[16], M. Santander[14], G. H. Sembroski[11], K. Shahinyan[16], D. Staszak[25], I. Telezhinsky[8,9], J. V. Tucci[11], J. Tyler[2], S. P. Wakely[25], O. M. Weiner[20], A. Weinstein[13], A. Wilhelm[8,9], D. A. Williams[21]
(VERITAS Collaboration),
and
S. Fegan[27], B. Giebels[27], D. Horan[27]
(*Fermi*-LAT Collaboration),
A. Berdyugin[28], J. Kuan[20], E. Lindfors[28], K. Nilsson[29], A. Oksanen[30], H. Prokoph[31], R. Reinthal[28], L. Takalo[28], and F. Zefi[27]
[1] Department of Physics and Astronomy, University of Utah, Salt Lake City, UT 84112, USA
[2] Physics Department, McGill University, Montreal, QC H3A 2T8, Canada
[3] Department of Physics, Washington University, St. Louis, MO 63130, USA; errando@physics.wustl.edu
[4] Fred Lawrence Whipple Observatory, Harvard-Smithsonian Center for Astrophysics, Amado, AZ 85645, USA
[5] School of Physics, University College Dublin, Belfield, Dublin 4, Ireland
[6] Department of Physics and Astronomy, University of California, Los Angeles, CA 90095, USA
[7] Argonne National Laboratory, 9700 S. Cass Avenue, Argonne, IL 60439, USA
[8] Institute of Physics and Astronomy, University of Potsdam, D-14476 Potsdam-Golm, Germany
[9] DESY, Platanenallee 6, D-15738 Zeuthen, Germany
[10] Astronomy Department, Adler Planetarium and Astronomy Museum, Chicago, IL 60605, USA
[11] Department of Physics and Astronomy, Purdue University, West Lafayette, IN 47907, USA
[12] Department of Physics and Center for Astrophysics, Tsinghua University, Beijing 100084, China
[13] Department of Physics and Astronomy, Iowa State University, Ames, IA 50011, USA
[14] Department of Physics and Astronomy, Barnard College, Columbia University, NY 10027, USA; muk@astro.columbia.edu
[15] Department of Astronomy and Astrophysics, 525 Davey Lab, Pennsylvania State University, University Park, PA 16802, USA
[16] School of Physics and Astronomy, University of Minnesota, Minneapolis, MN 55455, USA
[17] Department of Physics, California State University—East Bay, Hayward, CA 94542, USA
[18] School of Physics, National University of Ireland Galway, University Road, Galway, Ireland
[19] Department of Physics and Astronomy and the Bartol Research Institute, University of Delaware, Newark, DE 19716, USA
[20] Physics Department, Columbia University, New York, NY 10027, USA
[21] Santa Cruz Institute for Particle Physics and Department of Physics, University of California, Santa Cruz, CA 95064, USA
[22] Department of Physics and Astronomy, University of Iowa, Van Allen Hall, Iowa City, IA 52242, USA
[23] Department of Physics and Astronomy, DePauw University, Greencastle, IN 46135-0037, USA
[24] School of Physics and Center for Relativistic Astrophysics, Georgia Institute of Technology, 837 State Street NW, Atlanta, GA 30332-0430, USA
[25] Enrico Fermi Institute, University of Chicago, Chicago, IL 60637, USA
[26] Department of Physical Sciences, Cork Institute of Technology, Bishopstown, Cork, Ireland
[27] Laboratoire Leprince-Ringuet, Ecole polytechnique, CNRS/IN2P3, Université Paris-Saclay, F-91128, Palaiseau, France; sfegan@llr.in2p3.fr, zefi@llr.in2p3.fr
[28] Tuorla Observatory, Department of Physics and Astronomy, University of Turku, Finland
[29] Finnish Centre for Astronomy with ESO, University of Turku, Finland
[30] Nyrola observatory, Jyvaskylan Sirius ry, Finland
[31] Department of Physics and Electrical Engineering, Linnaeus University, SE-351 95 Växjö, Sweden
Received 2016 July 11; revised 2016 December 28; accepted 2017 January 4; published 2017 February 21

Abstract

B2 1215+30 is a BL-Lac-type blazar that was first detected at TeV energies by the MAGIC atmospheric Cherenkov telescopes and subsequently confirmed by the Very Energetic Radiation Imaging Telescope Array System (VERITAS) observatory with data collected between 2009 and 2012. In 2014 February 08, VERITAS detected a large-amplitude flare from B2 1215+30 during routine monitoring observations of the blazar 1ES 1218 +304, located in the same field of view. The TeV flux reached 2.4 times the Crab Nebula flux with a variability timescale of <3.6 hr. Multiwavelength observations with *Fermi*-LAT, *Swift*, and the Tuorla Observatory revealed a correlated high GeV flux state and no significant optical counterpart to the flare, with a spectral energy distribution where the gamma-ray luminosity exceeds the synchrotron luminosity. When interpreted in the framework of a one-zone leptonic model, the observed emission implies a high degree of beaming, with Doppler factor $\delta > 10$, and an electron population with spectral index $p < 2.3$.

Key words: BL Lacertae objects: individual (B2 1215+30, VER J1217+301) – galaxies: active – galaxies: jets – galaxies: nuclei – gamma rays: galaxies

Table 1
Summary of the VERITAS and *Fermi*-LAT Results from Observations of B2 1215+30 in Different Epochs

Instrument	Energy Range	Dates	Live Time (minutes)	Significance	Flux ($cm^{-2}\,s^{-1}$)
VERITAS	>0.2 TeV	2013 Jan 06–2013 May 12 (MJD 56,298–56,424)	631	8.8σ	$(6.0 \pm 1.2) \times 10^{-12}$
		2013 Feb 07 (MJD 56,330)	25	10.5σ	$(5.1 \pm 1.0) \times 10^{-11}$
		2014 Jan 29–2014 May 25 (MJD 56,686–56,802)	748	23.6σ	$(2.4 \pm 0.2) \times 10^{-11}$
		2014 Feb 08 (MJD 56,696)	45	46.5σ	$(5.0 \pm 0.1) \times 10^{-10}$
		2014 Feb 09 (MJD 56,697)	25	1.6σ	$<1.4 \times 10^{-11}$
Fermi-LAT	0.1–500 GeV	2013 Jan 06–2013 May 12 (MJD 56,298–56,424)		28.8σ	$(6.8 \pm 0.7) \times 10^{-8}$
		2014 Jan 01–2014 May 25 (MJD 56,658–56,802)		34.5σ	$(1.0 \pm 0.1) \times 10^{-7}$
		2014 Feb 05–2014 Feb 09 (MJD 56,693–56,696)		17.4σ	$(4.4 \pm 0.7) \times 10^{-7}$

Note. The VERITAS upper limit is computed at 95% c.l. Here we assume a power-law spectrum with index $\Gamma = 3.0$.

1. Introduction

Extreme flux variability is one of the defining properties of the blazar class of active galactic nuclei, appearing at all wavelengths over a wide range of timescales. Flares with amplitudes up to 100 times the quiescent flux and variability timescales as short as 3 minutes have been observed at TeV energies ($E \gtrsim 0.1$ TeV; see, e.g., Aharonian et al. 2007). To date, six flaring BL-Lac-type blazars have been detected to exceed the flux of the Crab Nebula (1 Crab $= (2.1 \pm 0.2) \times 10^{-10}\,cm^{-2}\,s^{-1}$ at $E > 0.2$ TeV; Hillas et al. 1998) at TeV energies. The large signal statistics obtained during bright flares enable flux-variability studies on minute timescales, resulting in tighter constraints on the size and location of the gamma-ray-emitting region (see, e.g., Begelman et al. 2008) and probing the particle acceleration and cooling mechanisms in blazar jets (see, e.g., Bykov et al. 2012).

This paper describes a large-amplitude gamma-ray flare from the blazar B2 1215+30 detected on UT date 2014 February 08 and compares its broadband properties to long-term observations of the source with the Very Energetic Radiation Imaging Telescope Array System (VERITAS; TeV energies), *Fermi*-LAT (GeV energies; $0.1 \lesssim E \lesssim 100$ GeV), and the Tuorla optical observatory.

B2 1215+30 (R.A. $= 12^h17^m52^s$, decl. $= +30°07'00''1$, J2000), also known as ON 325 or 1ES 1215+303, was first detected at TeV energies by MAGIC (Aleksić et al. 2012). At GeV energies it is associated with 3FGL J1217.8+3007 (Acero et al. 2015). There is some uncertainty in the distance to this source, with values of $z = 0.130$ (Akiyama et al. 2003) and $z = 0.237$ (Lanzetta et al. 1993) being quoted for its spectroscopic redshift. Based on the location of its synchrotron peak, B2 1215+30 has been classified as either an intermediate (IBL; Nieppola et al. 2006) or a high-frequency peaked BL Lac (HBL; Ackermann et al. 2015).

Throughout this paper we assume a Friedmann universe with $H_0 = 67.7\,km\,s^{-1}\,Mpc^{-1}$, $\Omega_m = 0.309$, and $\Omega_\Lambda = 0.691$. All distance-dependent quantities are calculated assuming a redshift $z = 0.130$ ($d_L = 630$ Mpc) for B2 1215+30. Measurement uncertainties are statistical only unless indicated otherwise.

2. VERITAS Observations

VERITAS is an array of four imaging atmospheric Cherenkov telescopes located at the Fred Lawrence Whipple Observatory in southern Arizona, USA. VERITAS operates by recording Cherenkov light from particle showers initiated by gamma rays in the upper atmosphere and is sensitive to gamma-ray energies from about 85 GeV to more than 30 TeV (Park 2015).

Table 1 summarizes the VERITAS observations and results on B2 1215+30. Observations were made in "wobble" pointing mode (Fomin et al. 1994) considering the presence of another TeV source in the field of view (1ES 1218+304, offset 0°.76 from B2 1215+30), as described in Aliu et al. (2013). Data were processed using standard VERITAS analysis pipelines (Acciari et al. 2009; Archambault et al. 2013). The energy threshold of the analysis is 200 GeV, with a systematic uncertainty of 20% on the energy estimation.

A TeV flare from B2 1215+30 was detected in 2013 February 07 (MJD 56,330; Figure 1) with flux $F_{>0.2\,TeV} = (5.1 \pm 1.0_{stat} \pm 1.0_{sys}) \times 10^{-11}\,cm^{-2}\,s^{-1}$, or 0.24 Crab. The measured gamma-ray spectrum is compatible with a power law ($dN/dE = N_0 \cdot E^{-\Gamma}$) with photon index $\Gamma = 3.7 \pm 0.7_{stat} \pm 0.4_{sys}$, in line with $\Gamma = 3.6 \pm 0.4$ reported in Aliu et al. (2013) and $\Gamma = 3.0 \pm 0.1$ from Aleksić et al. (2012). A fit of the decaying phase of the flare (MJD 56,330–56,639) to a function $F(t) = F_0(1 + 2^{-(t-t_0)/t_{var}})$ results in an upper limit on the flux halving time of $t_{var} < 52$ hr at a 90% confidence level (c.l.).

A brighter subsequent flare from B2 1215+30 was observed on 2014 February 08 (MJD 56,696; Figure 1) with flux $F_{>0.2\,TeV} = (5.0 \pm 0.1_{stat}\,^{+4.0_{sys}}_{-1.0_{sys}}) \times 10^{-10}\,cm^{-2}\,s^{-1}$, or 2.4 Crab. The reconstructed energy spectrum is compatible with a power law with photon index $\Gamma = 3.1 \pm 0.1_{stat} \pm 0.6_{sys}$ between 0.2 and 2 TeV (Figure 2). The observations targeted 1ES 1218+304 and had a mean zenith distance of 27°, accumulating 45 minutes of live-time exposure. On that night, a high-cloud layer at an altitude of 11.2 km a.s.l. was measured by an on-site Vaisala CL51 ceilometer. On average, 30% of the Cherenkov light output in particle showers initiated by 200 GeV gamma rays is produced above 11.2 km (see, e.g., Rossi & Greisen 1941). This fraction decreases with increasing gamma-ray energy (see, e.g., Weekes 2003, p. 11). If all Cherenkov light emitted above the cloud layer is lost, VERITAS would underestimate the energy of incoming gamma rays by ~30%, which, added to the 20% systematic uncertainty on the energy estimation, results in the increased systematic error on the gamma-ray flux and spectral index measured in 2014 February 08. The large signal statistics during the flare allow flux measurements in 5-minute time bins (Figure 3). No significant flux variability was detected during the 45-minute exposure, with the light curve deviating from a constant flux hypothesis at a level of 2.8 standard deviations. Observations on the next night (2014 February 09) did not show an elevated flux from

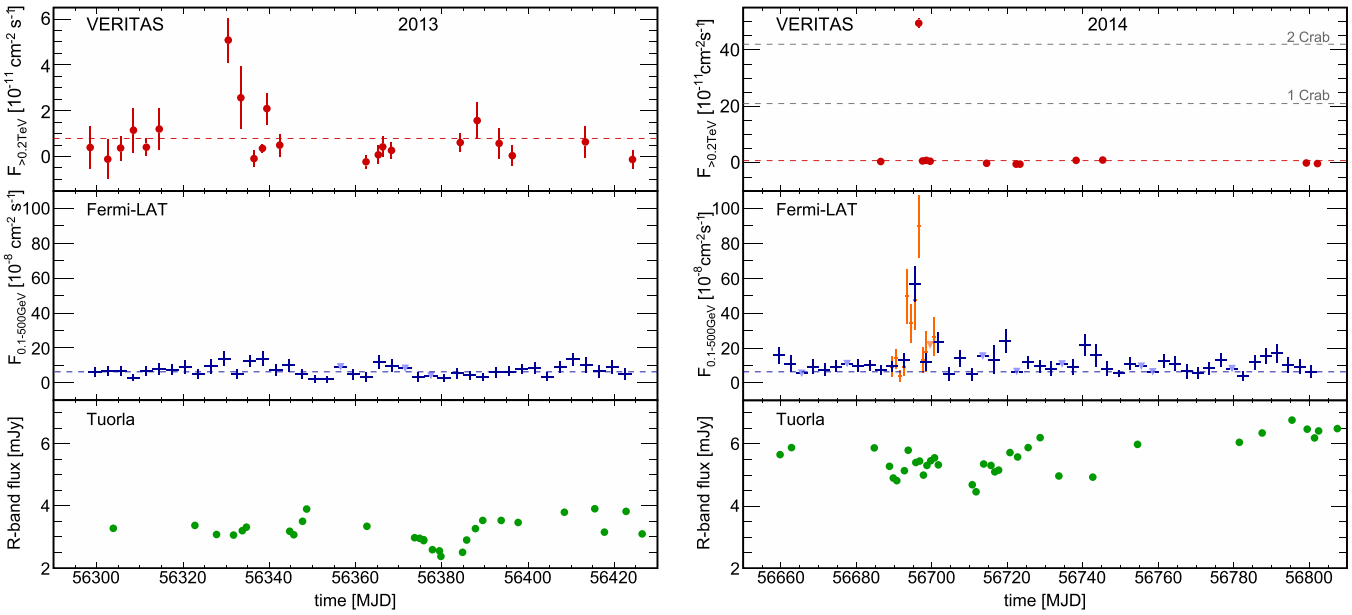

Figure 1. TeV (top), GeV (middle), and optical (bottom) light curves of B2 1215+30 in 2013 (left panels) and 2014 (right panels). Fluxes are calculated in 1-day bins for VERITAS. *Fermi*-LAT fluxes are calculated with 3-day integration bins (blue plus signs) and 1-day bins (orange plus signs) around the time of the 2014 flare. Downward-pointing triangles indicate 95% c.l. upper limits derived from the *Fermi*-LAT data for time bins with signal smaller than 2σ. The yearly averaged TeV flux in 2011 (8.0×10^{-12} cm^{-2} s^{-1}; Aliu et al. 2013) is shown by a red dashed line, and a blue dashed line indicates the average GeV flux from Acero et al. (2015). Statistical errors on the Tuorla optical fluxes are smaller than the data points.

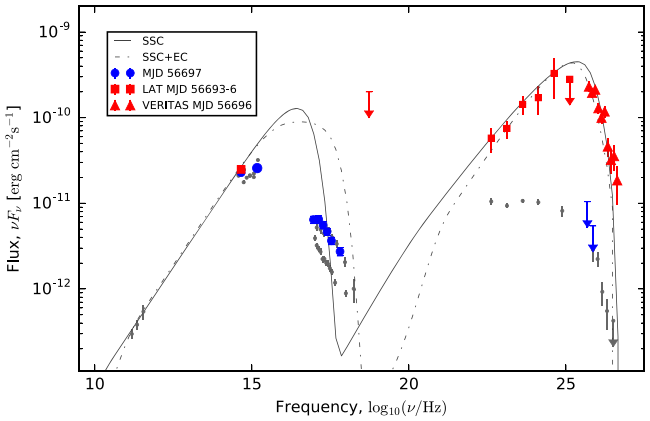

Figure 2. Broadband SED of B2 1215+30 at different epochs. Red markers show the state of the source during the 2014 February 08 flare, including VERITAS (MJD 56,696.52), *Fermi*-LAT (MJD 56,693–56,696), *Swift*-BAT (MJD 56,696), and Tuorla (MJD 56,696.72) data. Blue markers show *Swift*-XRT and UVOT fluxes and VERITAS 95% c.l. upper limits taken 24 hr after the flare. Gray markers show archival observations from Aliu et al. (2013). The numerical SSC and SSC+EC models described in Section 6 are shown with a solid and a dashed gray line, respectively. Gamma-ray absorption by the extragalactic background light is applied to the models following Finke et al. (2010).

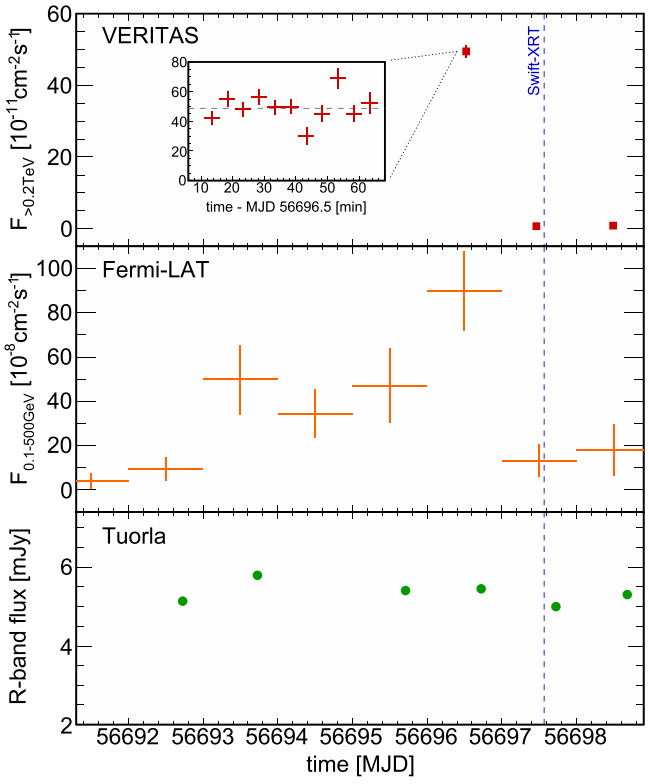

Figure 3. Same as Figure 1, but around the night of 2014 February 08 (MJD 56,696). The top panel inset shows the TeV flux on MJD 56,696 in 5-minute bins. A fit of the 5-minute-binned TeV light curve to a constant flux (gray dashed line) yields $P(\chi^2) = 4.2 \times 10^{-3}$. A vertical blue dashed line indicates the time of the *Swift*-XRT observation described in Section 4.

B2 1215+30 (Table 1), implying a 90% c.l. limit on the flux halving time of $t_{\rm var} < 3.6$ hr.

3. *Fermi*-LAT Observations

The Large Area Telescope (LAT) is a pair-conversion gamma-ray telescope on board the *Fermi* satellite covering energies from about 20 MeV to more than 500 GeV (Atwood et al. 2009). Table 1 summarizes the *Fermi*-LAT observations and results on B2 1215+30. Data were analyzed using the unbinned likelihood analysis in LAT ScienceTools (`v10r0p5`) with `P8R2_SOURCE_V6` instrument response functions, selecting photons with energy 100 MeV $< E <$ 500 GeV in a circular region of 10° radius centered on the position of

B2 1215+30. The energy spectrum of B2 1215+30 was modeled with a power law. Further analysis details and standard quality cuts followed Acero et al. (2015). Light curves were derived by dividing the data in bins of duration 1 and 3 days.

A clear flux peak is seen coinciding with the VERITAS-detected flare of 2014 February 08 (Figure 1), followed by a rapid decay that constrains the flux halving time to $t_{\rm var} < 8.9$ hr at 90% c.l. (Figure 3). The GeV spectrum shows some evidence of hardening (2.2σ), going from an averaged $\Gamma_{\rm GeV} = 1.92 \pm 0.04$ during the 2014 campaign to $\Gamma_{\rm GeV} = 1.70 \pm 0.09$ in the 4 days of highest GeV flux (MJD 56,693–56,696). In 2013, the LAT light curve shows no significant flux variability (Figure 1). However, the same TeV-to-GeV flare amplitude ratio seen in 2014 can be accommodated within the error bars of the 2013 LAT light curve.

4. *Swift* Observations

An observation by the *Swift* Observatory (ObsID 00031906012) was carried out 1 day after the VERITAS-detected flare (Figure 3), with an exposure of 1.97 ks. X-ray Telescope (XRT, 0.2–10 keV; Burrows et al. 2005) data were obtained in photon-counting mode and processed with the `xrtpipeline` tool (HEASOFT 6.16). The exposure shows a stable source-count rate of $\sim 0.3\ {\rm s}^{-1}$, suggesting negligible pileup effects.

The spectrum was rebinned to have at least 20 counts per bin, ignoring channels with energy below 0.3 keV, and fit using PyXspec v1.0.4 (Arnaud 1996). An absorbed power law with column density $N_{\rm H} = 1.68 \times 10^{20}\ {\rm cm}^{-2}$ (Kalberla et al. 2005) and photon index $\Gamma_{\rm X} = 2.54 \pm 0.07$ gives a good description of the spectral data ($P(\chi^2) = 0.42$). The unabsorbed flux is $F_{0.3-10\,{\rm keV}} = (1.28 \pm 0.05) \times 10^{-11}\ {\rm erg\ cm^{-2}\ s^{-1}}$.

To analyze the *Swift*-UVOT data ($E \sim 6.0$ eV), source counts were extracted from an aperture of $5\farcs0$ radius around the source. Background counts were taken from four neighboring regions with equal radius. Magnitudes were computed using the `uvotsource` tool (HEASOFT v6.16), corrected for extinction according to Roming et al. (2009) using $E(B-V)$ from Schlafly & Finkbeiner (2011), and converted to fluxes following Poole et al. (2008).

5. Optical Observations

Optical *R*-band data were obtained as part of the Tuorla blazar monitoring program (http://users.utu.fi/kani/1m; Takalo et al. 2008). Observations were taken using a 35 cm Celestron telescope attached to the KVA 60 cm telescope (La Palma, Canary Islands, Spain) and the 50 cm Searchlight Observatory Network telescope (San Pedro de Atacama, Chile). Data were analyzed using a semiautomatic pipeline developed at the Tuorla Observatory. The host galaxy flux of 1.0 mJy (Nilsson et al. 2007) was subtracted from the observed fluxes, and a correction for Galactic extinction was applied using values from Schlafly & Finkbeiner (2011). The yearly averaged optical flux of 3.27 ± 0.01 mJy in year 2013 is similar to historical values dating back to 2003.[32] In 2014, B2 1215+30 appeared to be in a long-lasting high optical state, with average flux of 5.56 ± 0.02 mJy. No significant enhancement of the optical emission was detected in coincidence with the two gamma-ray flares reported in Sections 2 and 3.

6. Discussion

With the data presented here and in Aliu et al. (2013), VERITAS has published TeV observations of B2 1215+30 spanning over 50 nights between 2008 and 2014, finding no significant deviations from yearly averaged fluxes other than the flares on 2013 February 07 and 2014 February 08 reported in this paper. These two TeV flares had amplitudes of ∼6 and ∼60 times the average quiescent flux from B2 1215+30, with associated flux halving times of ∼52 and ∼3.6 hr, respectively. Such large-amplitude, short-lived, isolated flares are not common in TeV-emitting blazars. Fast variability is typically measured during longer high-flux states in HBLs (see, e.g., Krawczynski et al. 2004; Albert et al. 2007), while some quasars and IBLs show short periods of TeV emission in epochs where multiple GeV flares are seen (Aleksić et al. 2011; Arlen et al. 2013).

In the following we summarize the main observational properties of the brightest flare of 2014 February 08 and interpret them in the framework of a homogeneous one-zone leptonic emission scenario:

(i) The measured flux above 0.2 TeV was $(5.0 \pm 0.1) \times 10^{-10}\ {\rm cm^{-2}\ s^{-1}}$. This corresponds to an isotropic luminosity $L_\gamma = 1.7 \times 10^{46}\ {\rm erg\ s^{-1}}$. To date, only four other blazars have episodically been observed to emit TeV radiation with luminosity exceeding $10^{46}\ {\rm erg\ s^{-1}}$. For comparison, the historical TeV blazar Mrk 421 would have to exhibit a 35 Crab flare to reach the luminosity of the B2 1215+30 outburst reported here.

(ii) A nondetection by VERITAS 24 hr after the flare indicates a flux halving time $t_{\rm var} < 3.6$ hr at TeV energies. Causality implies that the observed variability timescale is related to the size (R) and Doppler factor (δ) of the gamma-ray-emitting region by

$$R\delta^{-1} \leqslant c\, t_{\rm var}/(1+z) = 3.4 \times 10^{14}\ {\rm cm}. \quad (1)$$

(iii) The TeV flare was accompanied by a significant GeV flare measured by *Fermi*-LAT that extended over 4 days and displayed some evidence for spectral hardening, with $\Gamma_{\rm GeV} = 1.70 \pm 0.09$.

(iv) Optical observations did not show enhanced emission in coincidence with the GeV and TeV flare, although the overall optical flux in 2014 was approximately two times brighter than in previous years.

(v) Nondetections by *Swift*-BAT[33] (15–50 keV) and MAXI[34] (4–10 keV) on the day of the TeV flare (MJD 56,696) can be interpreted as a limit on the hard X-ray flux of the order of $\nu_{\rm x} F_{\nu_{\rm x}} \lesssim 2 \times 10^{-10}\ {\rm erg\ cm^{-2}\ s^{-1}}$ (Hiroi et al. 2013; Krimm et al. 2013). This effectively limits the peak synchrotron luminosity to

$$L_{\rm syn} \leqslant 10^{46}\ {\rm erg\ s^{-1}}. \quad (2)$$

(vi) No change in the 15 GHz radio brightness of B2 1215+30 was seen in the Owens Vally Radio Observatory (OVRO) light curves in coincidence with or after the TeV flare.[35] B2 1215+30 is in fact in the lower third of the OVRO sample in terms of radio flux variability (Richards et al. 2014).

[32] http://users.utu.fi/kani/1m/ON_325_jy.html

[33] http://swift.gsfc.nasa.gov/results/transients/weak/QSOB1215p303/

[34] http://maxi.riken.jp/mxondem/

[35] http://www.astro.caltech.edu/ovroblazars/data/data.php?page=data_return&source=J1217+3007

(vii) *Swift*-XRT data taken 24 hr after the flare showed an X-ray flux comparable with historical average values (Aleksić et al. 2012; Aliu et al. 2013), although the TeV flux was back to a quiescent level at that point.

A lower limit on δ can be derived by estimating the required Doppler boosting for gamma rays with energy E_γ to escape pair production on a co-spatial synchrotron photon field with density $F(E_0)$, where $E_0 = (m_e c^2)^2 (1+z)^{-2} \delta^2 E_\gamma^{-1}$. For photons with $E_\gamma \sim 1$ TeV measured by VERITAS the mean interaction energy for pair production is $E_0 = 76$ eV. Using the expression for optical depth from Dondi & Ghisellini (1995), imposing $\tau_{\gamma\gamma} \leqslant 1$, and estimating $F(E_0)$ from the *Swift*-XRT and UVOT measurements described in Section 4 results in

$$\delta \geqslant \left[\frac{\sigma_T d_L^2 (1+z)^{2\alpha}}{5hc^2} \frac{F(E_0)}{t_{var}} \right]^{1/(4+2\alpha)},$$
$$\delta \geqslant 10.0, \quad (3)$$

where σ_T is the Thomson cross section and α is the spectral index of the synchrotron emission around E_0. We note that the *Swift* observations were made 24 hr after the TeV flare (Figure 3). The lower limit on δ is still valid, however, as long as the density of synchrotron photons was not lower during the flare than that measured on the subsequent day.

The spectral energy distribution (SED) of B2 1215+30 during the flare is shown in Figure 2. TeV emission can be explained by a fresh injection of relativistic electrons, where the injected perturbation propagates down in energy as the plasma cools, explaining the smaller amplitude of the GeV flare and the lack of optical variability (see, e.g., Giebels et al. 2007). Taking the radio spectrum from Antón et al. (2004) and the *R*-band flux from the Tuorla Observatory, we derive a radio-to-optical spectral index $\alpha_{ro} = 0.45$. If the cooling break[36] in the synchrotron SED happens beyond optical frequencies, as assumed in Aleksić et al. (2012) and Aliu et al. (2013) and typically observed in BL Lac objects (Tavecchio et al. 2010), α_{ro} determines the power-law spectral index (p) of the emitting electrons (see, e.g., Rybicki & Lightman 1979):

$$p = 1 + 2\alpha_{ro} \approx 1.9. \quad (4)$$

Beyond the cooling break, the electron distribution has to extend to Lorentz factors (γ) of the order

$$\gamma_{max} \approx (1+z)\delta^{-1} \frac{1\ \mathrm{TeV}}{m_e c^2} \geqslant 2.2 \times 10^5 (\delta/10)^{-1} \quad (5)$$

to produce the ~1 TeV photons detected by VERITAS. In the simplest leptonic emission scenario, the high-energy component of the SED is produced via the synchrotron self-Compton mechanism (SSC; Maraschi et al. 1992). In an SSC scenario, the ratio between the synchrotron and inverse-Compton luminosities can be used to estimate the magnetic field. Following Ghisellini et al. (1996) and using Equations (2) and (3) to constrain L_{syn} and δ, we derive

$$B \simeq (1+z)\delta^{-3} \left(\frac{2L_{syn}^2}{L_\gamma c^3 t_{var}} \right)^{1/2},$$
$$\leqslant 1.8\ \mathrm{G} (L_{syn}/10^{46}\ \mathrm{erg\ s^{-1}}) (\delta/10)^{-3}. \quad (6)$$

The scarcity of multiwavelength coverage simultaneous with the TeV flare, especially of the synchrotron component, leaves numerical modeling of the SED underconstrained. However, even if modeling solutions are not unique, they can be used to understand the level of kinetic and magnetic jet power required under different scenarios. We test the feasibility of an SSC scenario by using the stationary leptonic model of Böttcher et al. (2013), fixing the jet viewing angle to δ^{-1} for simplicity. Models[37] within the parameter constraints from Equations (1) to (6) reproduce the measured gamma-ray luminosity without overproducing the optical flux measured by the Tuorla Observatory, and keeping $L_{syn} \lesssim L_\gamma$ as constrained by the *Swift*-BAT nondetection (Figure 2). These solutions would indicate an emitting region where the kinetic power of relativistic electrons (L_e) exceeds the power carried by the magnetic field (L_B) by a factor of ~1200. This is typically the case in SSC modeling of TeV blazars (see, e.g., Aliu et al. 2013). Higher values of δ would imply even higher L_e/L_B ratios. Given the observational uncertainty in the shape of the synchrotron emission, we also explore a wider range of electron spectral indices than indicated in Equation (4), finding that $p < 2.3$ is required to reproduce the hard GeV spectrum measured by *Fermi*-LAT.

The lack of observable thermal emission from the accretion disk and associated emission lines in B2 1215+30 supports an SSC emission scenario. However, the observed Compton dominance ($L_\gamma/L_{syn} \gtrsim 1$) typically points to external Compton models (EC; Dermer & Schlickeiser 1993) to explain the high-energy emission. Assuming an EC scenario, constraints on δ and the distance of the energy dissipation region from the black hole (r_{diss}) can be derived assuming reasonable limits on the jet collimation and luminosity of upscattered synchrotron photons. Following Nalewajko et al. (2014) results in

$$\delta(r_{diss}) < \left[\frac{(1+z) r_{diss}}{c\ t_{var}} \right]^{1/2}, \quad (7)$$

$$\delta(r_{diss}) > \left[\frac{9}{2} \frac{L_\gamma}{\zeta(r_{diss}) L_d} \right]^{1/8} \left[\frac{(1+z) r_{diss}}{2\ c\ t_{var}} \right]^{1/4}, \quad (8)$$

where the accretion disk luminosity (L_d) is assumed to be 4×10^{43} erg s^{-1} (Ghisellini et al. 2010) and $\zeta(r_{diss})$ describes the composition of the external radiation fields. Equations (7) and (8) constrain the (δ, r_{diss}) parameter space with a marginal solution at $\delta > 19$ and $r_{diss} > 1.2 \times 10^{17}$ cm that would place the emitting blob beyond the broad-line region. A numerical EC model[38] (Böttcher et al. 2013) with an external photon field described as blackbody emission with $T_{ext} = 10^3$ K typical of hot dust can reproduce the SED with $L_e/L_B \sim 1$ (Figure 2).

[36] Corresponding to emitting electron energies at which the radiative cooling and escape timescales are equal.

[37] For example, $L_e = 1.05 \times 10^{45}$ erg s^{-1}, $q_e = 1.9$, $\delta = \gamma_{min} = 40$, $\gamma_{max} = 10^5$, $B = 0.03$ G, $R = 1.3 \times 10^{16}$ cm, $\eta_{esc} = 1$; see Böttcher et al. (2013) for parameter definitions not included in the text.

[38] $L_e = 5 \times 10^{43}$ erg s^{-1}, $q_e = 1.9$, $\delta = \gamma_{min} = 40$, $\gamma_{max} = 10^5$, $B = 0.3$ G, $R = 10^{16}$ cm, $u_{ext} = 2 \times 10^{-6}$ erg cm^{-3}, $T_{ext} = 10^3$ K, $\eta_{esc} = 1$; see Böttcher et al. (2013) for parameter definitions not included in the text.

Particle acceleration in relativistic shocks or through magnetic reconnection can explain the short flux-variability timescale observed in B2 1215+30 (Sironi & Spitkovsky 2009; Giannios 2013). The hard electron spectrum ($p \lesssim 2.3$) derived from the multiwavelength SED is usually obtained in semianalytical calculations of relativistic shock acceleration (Achterberg et al. 2001), but more recent fully kinetic particle-in-cell simulations derive significantly softer spectra (Sironi & Spitkovsky 2009). Magnetic reconnection events can produce harder electron spectra than those originating from shock acceleration (Sironi & Spitkovsky 2014), easily reproducing $p \sim 1.9$ derived from the synchrotron spectrum of B2 1215 +30. Recently, Sironi et al. (2015) have suggested that magnetic reconnection is a more viable scenario for particle acceleration in relativistic jets, disfavoring shock models for their inability to simultaneously dissipate energy and accelerate particles beyond thermal energies. Efficient magnetic reconnection requires an emitting region in rough equipartition between particles and magnetic field ($L_e/L_B \lesssim 1$). The EC scenario presented above does fulfill this condition, while our attempts to describe the observed SED with SSC models persistently resulted in particle-dominated emitting regions where the magnetization of the plasma would be too low for efficient magnetic reconnection to take place.

VERITAS will continue to monitor B2 1215+30. Events like the extreme flare of 2014 February 08 should be within the sensitivity reach of HAWC (Lauer & Younk 2015). Future observations will show how frequent these extreme gamma-ray flares are and whether or not they are present in the majority of TeV blazars.

The authors thank Markus Böttcher for valuable discussions about leptonic emission models and David Sanchez for providing useful comments on the draft. R.M. acknowledges support from the Alliance Program at École Polytechnique and Columbia University. VERITAS research is supported by grants from the U.S. Department of Energy Office of Science, the U.S. National Science Foundation, and the Smithsonian Institution, and by NSERC in Canada. We acknowledge the excellent work of the technical support staff at the Fred Lawrence Whipple Observatory and at the collaborating institutions in the construction and operation of the instrument. The VERITAS Collaboration is grateful to Trevor Weekes for his seminal contributions and leadership in the field of very high energy gamma-ray astrophysics, which made this study possible. The *Fermi*-LAT Collaboration acknowledges generous ongoing support from a number of agencies and institutes that have supported both the development and the operation of the LAT, as well as scientific data analysis. These include the National Aeronautics and Space Administration and the Department of Energy in the United States; the Commissariat à l'Energie Atomique and the Centre National de la Recherche Scientifique/Institut National de Physique Nucléaire et de Physique des Particules in France; the Agenzia Spaziale Italiana and the Istituto Nazionale di Fisica Nucleare in Italy; the Ministry of Education, Culture, Sports, Science and Technology (MEXT), the High Energy Accelerator Research Organization (KEK), and Japan Aerospace Exploration Agency (JAXA) in Japan; and the K. A. Wallenberg Foundation, the Swedish Research Council, and the Swedish National Space Board in Sweden. Additional support for science analysis during the operations phase is gratefully acknowledged from the Istituto Nazionale di Astrofisica in Italy and the Centre National d'Ètudes Spatiales in France. Support for this work was provided by NASA through grants HST-GO-13753 and by the Space Telescope Science Institute, which is operated by AURA, Inc., under NASA contract NAS 5-26555. The HST data used in this article are available at the MAST archive (at 10.17909/T9XG63).

References

Acciari, V. A., Aliu, E., Aune, T., et al. 2009, ApJ, 707, 612
Acero, F., Ackermann, M., Ajello, M., et al. 2015, ApJS, 218, 23
Achterberg, A., Gallant, Y. A., Kirk, J. G., & Guthmann, A. W. 2001, MNRAS, 328, 393
Ackermann, M., Ajello, M., Atwood, W. B., et al. 2015, ApJ, 810, 14
Aharonian, F. A., Akhperjanian, A. G., Bazer-Bachi, A. R., et al. 2007, ApJL, 664, 71
Akiyama, M., Ueda, Y., Ohta, K., Takahashi, T., & Yamada, T. 2003, ApJS, 148, 275
Albert, J., Aliu, E., Anderhub, H., et al. 2007, ApJ, 669, 862
Aleksić, J., Alvarez, E. A., Antonelli, L. A., et al. 2012, A&A, 544, A142
Aleksić, J., Antonelli, L. A., Antoranz, P., et al. 2011, ApJL, 730, L8
Aliu, E., Archambault, S., Arlen, T., et al. 2013, ApJ, 779, 92
Antón, S., Browne, I. W. A., Marchã, M. J. M., Bondi, M., & Polatidis, A. 2004, MNRAS, 352, 673
Archambault, S., Arlen, T., Aune, T., et al. 2013, ApJ, 776, 69
Arlen, T., Aune, T., Beilicke, M., et al. 2013, ApJ, 762, 92
Arnaud, K. A. 1996, in ASP Conf. Ser. 101, XSPEC: The First Ten Years, ed. G. H. Jacoby & J. Barnes. (San Francisco, CA: ASP), 17
Atwood, W. B., Abdo, A. A., Ackermann, M., et al. 2009, ApJ, 697, 1071
Begelman, M. C., Fabian, A. C., & Rees, M. J. 2008, MNRAS, 384, L19
Böttcher, M., Reimer, A., Sweeney, K., & Prakash, A. 2013, ApJ, 768, 54
Burrows, D. N., Hill, J. E., Nousek, J. A., et al. 2005, SSRv, 120, 165
Bykov, A., Gehrels, N., Krawczynski, H., et al. 2012, SSRv, 173, 309
Dermer, C. D., & Schlickeiser, R. 1993, ApJ, 416, 458
Dondi, L., & Ghisellini, G. 1995, MNRAS, 273, 583
Finke, J. D., Razzaque, S., & Dermer, C. D. 2010, ApJ, 712, 238
Fomin, V. P., Stepanian, A. A., Lamb, R. C., et al. 1994, APh, 2, 137
Ghisellini, G., Maraschi, L., & Dondi, L. 1996, A&AS, 120, 503
Ghisellini, G., Tavecchio, F., Foschini, L., et al. 2010, MNRAS, 402, 497
Giannios, D. 2013, MNRAS, 431, 355
Giebels, B., Dubus, G., & Khélifi, B. 2007, A&A, 462, 29
Hillas, A. M., Akerlof, C. W., Biller, S. D., et al. 1998, ApJ, 503, 744
Hiroi, K., Ueda, Y., Hayashida, M., et al. 2013, ApJS, 207, 36
Kalberla, P. M. W., Burton, W. B., Hartmann, D., et al. 2005, A&A, 440, 775
Krawczynski, H., Hughes, S. B., Horan, D., et al. 2004, ApJ, 601, 151
Krimm, H. A., Holland, S. T., Corbet, R. H. D., et al. 2013, ApJS, 209, 14
Lanzetta, K. M., Turnshek, D. A., & Sandoval, J. 1993, ApJS, 84, 109
Lauer, R. J., Younk, P. W. & for the HAWC Collaboration 2015, arXiv:1508.04479
Maraschi, L., Ghisellini, G., & Celotti, A. 1992, ApJL, 397, L5
Nalewajko, K., Begelman, M. C., & Sikora, M. 2014, ApJ, 789, 161
Nieppola, E., Tornikoski, M., & Valtaoja, E. 2006, A&A, 445, 441
Nilsson, K., Pasanen, M., Takalo, L. O., et al. 2007, A&A, 475, 199
Park, N. 2015, in Proc. ICRC, Performance of the VERITAS Experiment (Hague, The Netherlands), 771
Poole, T. S., Breeveld, A. A., Page, M. J., et al. 2008, MNRAS, 383, 627
Richards, J. L., Hovatta, T., Max-Moerbeck, W., et al. 2014, MNRAS, 438, 3058
Roming, P. W. A., Koch, T. S., Oates, S. R., et al. 2009, ApJ, 690, 163
Rossi, B., & Greisen, K. 1941, RvMP, 13, 240
Rybicki, G. B., & Lightman, A. P. 1979, Radiative Processes in Astrophysics (New York: Wiley-Interscience), 393
Schlafly, E. F., & Finkbeiner, D. P. 2011, ApJ, 737, 103
Sironi, L., Petropoulou, M., & Giannios, D. 2015, MNRAS, 450, 183
Sironi, L., & Spitkovsky, A. 2009, ApJ, 698, 1523
Sironi, L., & Spitkovsky, A. 2014, ApJL, 783, L21
Takalo, L. O., Nilsson, K., Lindfors, E., et al. 2008, in AIP Conf. Ser. 1085, Tuorla Blazar Monitoring Program (Melville, NY: AIP), 705
Tavecchio, F., Ghisellini, G., Ghirlanda, G., Foschini, L., & Maraschi, L. 2010, MNRAS, 401, 1570
Weekes, T. 2003, Wiley Praxis Series in Astronomy and Astrophysics (Bristol: IOP)